THE ASTROPHYSICAL JOURNAL, Vol. 160, May 1970

ROCKET SPECTROSCOPY OF ZETA PUPPIS

ANDREW M. SMITH
Goddard Space Flight Center, National Aeronautics and Space Administration,
Greenbelt, Maryland
Received 1969 October 6; revised 1969 November 17

ABSTRACT

A spectrum of ζ Pup extending from 920 to 1360 Å with approximately 0.8 Å resolution has been recorded at rocket altitudes. Tentative identification of 102 multiplets of both stellar and interstellar origin has been made, from which it is concluded that all lines included in existing model atmospheres have been detected with the exception of those masked by telluric N_2 or strong P Cygni–type profiles. Additional weak absorption lines indicate a wide range of ionization and excitation entirely consistent with observations in the visible spectral region of stars of similar type; they also appear to affect sensibly the energy distribution within the spectrum. Transitions in C III (1176 Å), N III (990, 992 Å), N IV (955 Å), N V (1239, 1243 Å), O IV (1339, 1343 Å), O VI (1032, 1038 Å), and S VI (933, 944 Å) have been observed as P Cygni profiles. Except for the S VI lines, the mean radial velocities associated with ground-state transitions and the transition from the lowest triplet state in C III are close to an average velocity of 1770 km sec^{-1}; the mean radial velocities of the N IV and O IV ions are 530 and 150 km sec^{-1}, respectively. These results suggest a positive velocity gradient in the observed portion of the circumstellar envelope, and they also suggest that the escaping ions are loosely bound together with essentially no difference in their average acceleration away from the star. The interstellar columnar density of atomic hydrogen was found to be $(7.6 \pm 2.5) \times 10^{19}$ cm^{-2}, the quoted uncertainty being due only to the uncertainty in establishing the continuum. The mean atom density becomes $(6.4 \pm 2.1) \times 10^{-2}$ cm^{-3} if an interstellar distance through atomic hydrogen of 390 pc is assumed.

I. INTRODUCTION

In 1968 March the ultraviolet spectrum of ζ Pup (O5f) was recorded at rocket altitudes with wavelength coverage extending from 921 to 1360 Å at about 0.8 Å resolution. Presented in this paper are the results which have been discussed with the following objectives in mind.

1. It is desirable to establish the degree of consistency between the observed weak lines and those appearing in the visual spectra of stars of similar type.
2. A comparison between the observed strong ultraviolet lines and those included in existing model atmospheres for O5 stars may be made, particularly with a view to estimating the sufficiency of the model lines to account adequately for line blanketing.
3. P Cygni–type profiles may be examined with the hope of extracting more information about the circumstellar envelope.
4. Interstellar lines can be identified, but with the exception of the Lα line they cannot be reliably analyzed. A determination of the columnar density of atomic hydrogen can be made, and the result, contingent upon the value of the interstellar distance through atomic hydrogen, can be compared with a model of the interstellar medium.

II. THE EXPERIMENT

The instrumental payload was nearly identical with that described previously (Smith 1969), with substantial improvements being made only in the pointing control system. Briefly, the spectrograph itself consisted of a single, concave objective grating used in the so-called Wadsworth mount configuration with the characteristics listed in Table 1.

Kodak Pathé SC5 film was used, and the development procedure included slight agitation of the exposed film for 2 minutes in D198B at 68° F. A calibration curve is presented in Figure 1 in which the log of the exposure is plotted along the abscissa, and the film density averaged over the densitometer slit height is plotted on the ordinate. In deriving the calibration curve the assumption was made that there was no reciprocity failure at the short wavelengths of this experiment (Fowler, Rense, and Simmons 1965). This assumption permitted holding the source intensity constant while varying the exposure time and thus greatly simplified the calibration procedure. It should be noted that, though the slope of the calibration curve seemed to be relatively constant for different film samples and throughout the recorded wavelength range, the location of the curve along the exposure axis varied by as much as a factor of 2. The spread of data points about the solid curve gives an indication of the uncertainty involved in the instrument calibration. If it is assumed, however, that the calibration is sufficiently accurate to find the Lα line profile, then for this purpose the dynamic range of the instrument is about a factor of 5.

The payload was launched by an Aerobee 150 rocket from White Sands, New Mexico, on 1968 March 21 at 20:24 MST. Two exposures were secured, one at a mean altitude of 190 km for 214 sec, and another at 123 km for 68 sec. The fluctuation of the pointing direction about the line between the Earth and the star was within ± 11 seconds of arc both in the plane and normal to the plane of dispersion. This was achieved by the STRAP III attitude control system provided by the Goddard Space Flight Center.

TABLE 1

ROCKET SPECTROGRAPH CHARACTERISTICS

Variable	Value
Focal length	24.9 cm
Grating size (aperture)	2 cm $\times$ 7 cm
Grating line density	1200 mm^{-1}
Grating coating	Pt
Field of view normal to dispersion plane	$\pm 0\overset{\circ}{.}5$
Field of view in dispersion plane	$\pm 1\overset{\circ}{.}0$
Laboratory resolution at 1134 Å	0.25 Å
Plate factor ($\sim$linear)	33.4 Å mm^{-1}

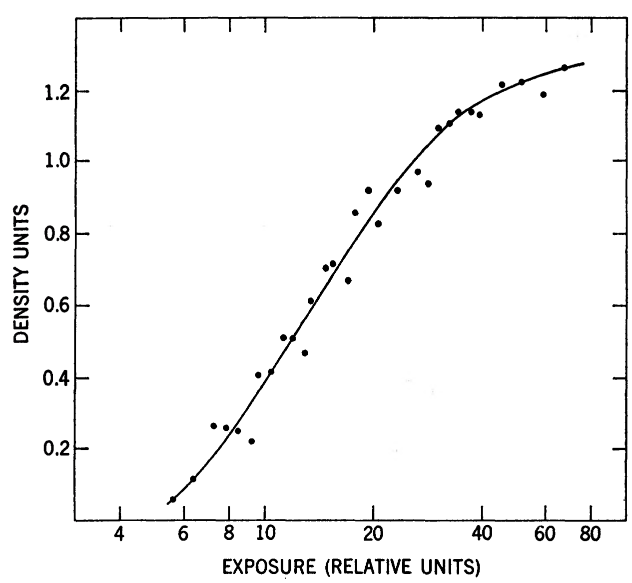

FIG. 1.—Calibration function of the rocket spectrograph. *Abscissa*, log of the exposure to Lα light in relative units; *ordinate*, film density averaged over the densitometer slit height.

Upon development of the flight film it was found that the second and short exposure possessed a background fog, most certainly arising from a light leak, which became progressively denser with decreasing wavelength. For this spectrogram the signal is still discernible at $\lambda > 990$ Å, but is used only at $\lambda > 1200$ Å principally to verify strong features identified on the long-exposure spectrogram for which background fog, if any, is indistinguishable from clear plate noise. The wavelength scale for the long exposure was determined by fitting the identified features produced by telluric N_2 ($\sim$960 Å), interstellar N I (1134.6 Å), and interstellar Si II (1304.4 Å) to a quadratic function of the distance measured on the film along the spectrum from an arbitrary starting point. The resulting scale is thought to be accurate within 0.3 Å. The resolution of the spectrograms is 0.8 Å or perhaps slightly better (0.7 Å), and limited by the pointing fluctuations.

III. RESULTS

An enlarged reproduction of both spectrograms appears in Figure 2 (Plate 5) with the strongest features identified. Figure 3 contains in three sections the microdensitometer traces of both spectrograms which have been smoothed in a computer by using a triangular weighting function of 0.62 Å full width at half-maximum. In Figure 2 and in Figure 3 at $\lambda > 1224$ Å data from the short exposure appear above the data of the long exposure, and the effect of the background fog in the former can easily be seen. The multiplets shown in Figure 3 include at least one transition which correlates with an observed spectral feature. Generally, all transitions of a given multiplet are indicated, but in a few cases some members have been excluded for purposes of clarity. The top spectrum appearing in Figure 3 corresponds to the model calculations of Hickok and Morton (1968) with $T_e = 37450°$ K and $\log g = 4.00$. In this case the ordinate is in flux units.

There are some features in the observed spectra which can be attributed to constituents of the Earth's atmosphere or, as in the case of water vapor, of the residual gas in the vicinity of the rocket during flight. As reported in an earlier observation of α Vir (Smith 1969), the absorption bands of N_2 are very strong at wavelengths less than 1000 Å, those near 960, 966, and 972 Å being particularly obvious. In fact, it seemed in the present case that these bands were chiefly responsible for the shape of the spectrum in this region, and were therefore used in the determination of the wavelength scale. The molecule O_2 also possesses absorption bands at these short wavelengths, specifically at 939, 948, 956, 966, 972, and 983 Å, but those of N_2 are expected to be stronger. An O_2 band at 1244 Å should, however, be seen in the short exposure at relatively low altitudes. Unfortunately, the data quality is poor, but a N V emission feature appearing in the long exposure at 1243 Å is missing in the short exposure, and the absence may be due to absorption from O_2 at this wavelength. The resonant line of O I at 1302.2 Å is present in the spectrum and may originate in the Earth's atmosphere. However, the two other lines of this triplet (1304.9 and 1306.0 Å), which should be observable if indeed the absorption is telluric, cannot be plausibly correlated with any observed feature. Thus, at least most of the observed 1302.2 Å absorption is thought to have an interstellar origin.

The features at 1018, 1056, 1113, and 1220 Å are attributed to absorption bands of H_2O adsorbed on the rocket and payload surfaces while on the ground and at low altitudes, and evaporated into the optical environment at the exposure altitudes.

It should be remarked that the emissionlike feature in the center of the Lα line of the long exposure is a film blemish, and can be seen as such in the spectrogram reproduction of Figure 2. Finally, in the long exposure the increase in intensity culminating in a sharp peak near 1327 Å is thought to be spurious, particularly in view of the fact that such behavior does not occur in the short exposure. There is also a film blemish in the neighborhood of this feature in the long exposure which might have extended into the spectrum thereby influencing the densitometer reading.

The identified spectral lines are listed in Table 2. Column (1) contains the ion identification, together with a multiplet or line reference. Regarding the latter, a number refers

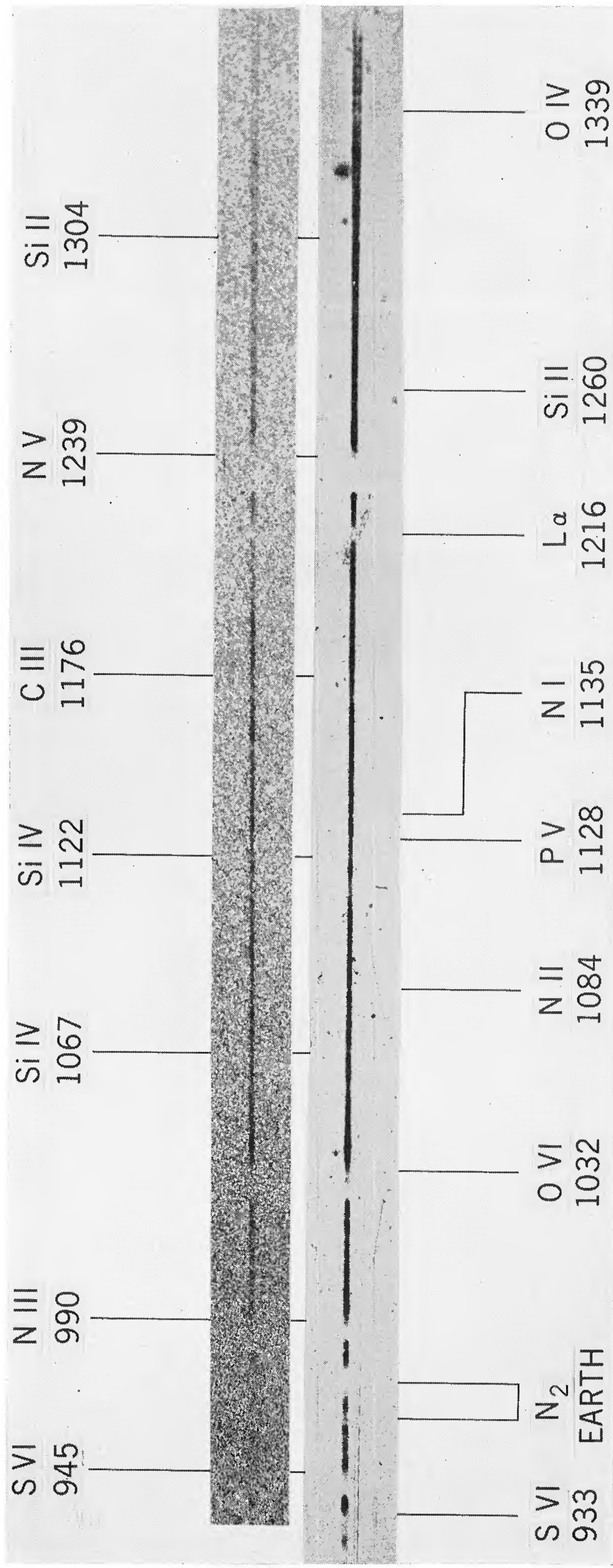

Fig. 2.—Two ultraviolet spectrograms of ζ Pup. Exposure times of the top and bottom spectrograms were 68 and 214 sec, respectively. Some identifications of the stronger features are shown, the numbers indicating the approximate wavelengths in angstroms.

Smith (*see* page 597)

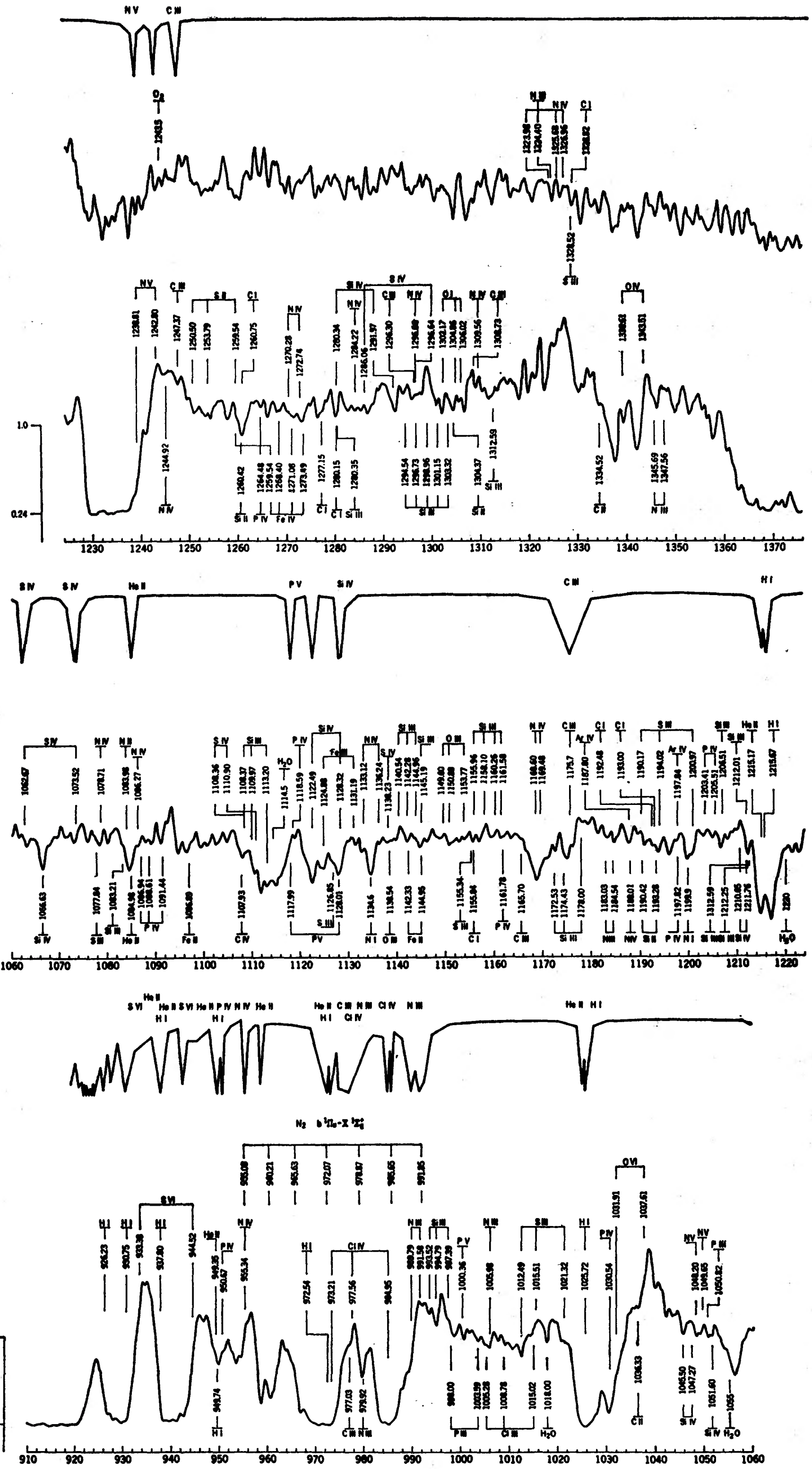

FIG. 3.—Microdensitometer traces in three sections of the ζ Pup spectrograms. Abscissae are in angstroms; ordinates represent densities of the 214-sec exposure which appears at the bottom of each section. A density of 0.24 corresponding to the background value is indicated. Top spectrum in each section corresponds to the model calculations of Hickok and Morton (1968); the ordinates (not shown) are in relative flux units. At λ > 1224 Å a trace of the 68-sec exposure spectrogram is shown between that of the 214-sec exposure and the model spectrum.

Table 2

Identifications of Lines in the UV Spectrum of Zeta Puppis

Ion Multiplet	λ(Å) Laboratory	λ(Å) Measured	χ(ev)	gf
H I	949.74	949.9	0.00	0.02788
(4) *m				
H I	1215.67	1215.9	0.00	0.8324
(1) s				
He II	949.30	949.9	40.64	0.030808
(19) ⁄,w,l	949.35			
He II	1084.91	1084.3	40.64	0.35736
(14) m	1084.98			
C I	1155.84	1155.8	0.00	---
(19) ∤,i,v,p	1156.06			
C I	1192.48	1192.9	0.00	---
(12) i,v,p				
C I	1192.92	1192.9	0.00	---
(11) i,v,p	1193.00			
C I	1260.75	1260.6	0.00	0.029
(9) i,m,p				
C I	1277.15	~1277	0.00	0.064
(7) i,w,l				
C I	1280.15	1280.1	0.00	0.020
(5) i,w,l				
C I	1328.82	1328.8	0.00	0.039
(4) i,w,p				
C II	1036.33	1036.3	0.00	0.12
(2) i,w,l				
C II	1334.52	1334.4	0.00	0.52
(1) i,w,l				
C III	977.03	~ 977	0.00	0.81
(1) w,l				
C III	1165.70	1165.7	22.62	---
(K) v,p	1165.87			
C III	1174.92		6.46	0.33
(4) c	1175.25		6.46	0.26
	1175.57	1168.8	6.46	0.20
	1175.70	1176.7	6.47	1.00
	1175.97		6.46	0.26
	1176.35		6.47	0.32
C III	1247.37	1247.2	12.64	0.27
(9) w,l				
C III	1296.30	1296.0	33.33	---
(K) w,p				
C III	1308.73	1309.0	22.62	---
(K) v,p				
C IV	1107.60	1108.0	39.51	---
(K) w,p	1107.93			
N I	1134.17		0.00	0.096
(2) i,m	1134.42	1134.6	0.00	0.19
	1134.98		0.00	0.26
N I	1199.55		0.00	0.72
	1200.22	1200.3	0.00	0.44
	1200.71		0.00	0.24
N II	1083.98	1084.3	0.00	0.17
(1) i,m	1084.57		0.01	0.13
	1084.57		0.01	0.39
	1085.54		0.02	0.12
	1085.70		0.02	0.70
N III	979.77		12.47	0.08
(12) w,l	979.84	979.7	12.47	0.72
	979.92		12.47	1.12
	980.01		12.47	0.08
N III	989.79	985.0	0.00	0.36
(1) c	991.51	990.3	0.02	0.07
	991.58		0.02	0.65
N III	1005.98	1005.9	16.17	0.36
(17) w,l	1006.03			0.18
N III	1183.03	1183.3	18.01	0.12
(20) w,p	1183.03		18.01	0.24
	1184.54	1184.8	18.02	0.12
	1184.54		18.02	0.60
N III	1324.40	1324.7	32.99	---
(K) w,p				
N III	1345.69	1346.2	2.72	---
(K) w,p	1346.27		2.71	---
	1347.56	---	2.73	---
N IV	955.34	953.8	16.13	0.22
(8) c		955.3		

Multiplet	λ(Å) Laboratory	λ(Å) Measured	χ(ev)	gf
N IV	1078.71	1078.4	52.98	---
(K) w,p				
N IV	1086.08	---	50.11	---
(K) v,p	1086.27	1086.3	50.12	---
	1086.69		50.12	---
N IV	1133.14	1132.9	46.57	---
(K) w,p	1135.24	---	46.57	---
	1136.22	1136.4	46.57	---
N IV	1168.60		51.85	---
(K) m,p	1169.06	1168.8	51.85	---
	1169.48		51.85	---
N IV	1188.01	1187.8	48.00	---
(K) w,p				
N IV	1243.73	1244.5	61.71	---
(K) v,p	1244.92		61.71	---
N IV	1270.28	1270.0	50.11	---
(K) w,p	1272.16		50.11	---
	1272.74	1273.0	50.11	---
	1273.47		50.11	---
	1273.72		50.11	---
N IV	1284.22	1284.1	52.98	---
(K) v,p				
N IV	1296.60	1296.0	52.98	---
(K) w,p				
N IV	1309.56	1309.0	23.32	---
(K) v,p				
N IV	1323.98	1324.4	51.85	---
(K) v,p	1325.68	1326.6	51.85	---
	1326.96		51.85	---
N V	1048.20	1048.7	76.28	---
(HA) w,p				
N V	1049.65	1048.7	76.29	---
(HA) w,p				
N V	1238.81	1233.3	0.00	0.31
(1) c	1242.80	1241.8	0.00	0.16
O I	1302.17	1302.2	0.00	0.16
(2) i,w,l				
O III	1138.54	1138.0	26.07	---
(K) v,p				
O III	1149.60	1149.0	24.42	---
(K) v,p	1150.88	1150.8	24.42	---
	1150.77	1153.9	24.42	---
O IV	1338.61	1337.6	22.28	---
(P) c		---		
	1342.99	1342.2	22.31	---
	1343.51	1343.7	22.31	---
O VI	1031.91	1025.5	0.00	0.26
(1) c	1037.61	1030.3	0.00	0.13
		1034.2		
Si II	1190.42	1190.9	0.00	0.92
(5) i,w,p	1193.28	1193.7	0.00	2.00
Si II	1260.42	1260.6	0.00	3.6
(4) i,m				
Si II	1304.37	1304.3	0.00	0.34
(3) i,w,l				
Si III	993.52	993.6	6.54	0.20
(6) w,l	994.79	994.8	6.55	0.64
	997.39	997.3	6.58	1.00
Si III	1083.21	1083.1	15.15	---
(23) v,p				
Si III	1108.37	1108.0	6.54	0.40
(5) w,p	1109.94	1110.3	6.55	1.20
	1109.97		6.55	
	1113.17		6.58	
	1113.20		6.58	2.00
	1113.23		6.58	
Si III	1140.54		16.08	---
(32) w,p	1141.58	1142.1	16.10	---
	1142.28		16.10	---
	1142.31		16.13	---
	1144.96	1144.8	16.13	---
	1145.67		16.13	
Si III	1145.12		28.55	---
(41) w,p	1145.15		28.55	---
	1145.16	1144.8	28.55	---
	1145.18		28.55	---
	1145.19		28,55	---
	1145.22		28.55	

Table 2 (cont'd.)

Ion Multiplet	λ(Å) Laboratory	λ(Å) Measured	χ(ev)	gf
Si III	1155.00	---	16.08	---
(31) v,p	1155.96	1155.7	16.10	---
	1156.78	1156.9	16.10	---
	1158.10	---	16.10	---
	1160.26	1159.4	16.13	---
	1161.58	1161.3	16.13	---
Si III	1172.53	1172.6	16.08	---
(30) v,p	1174.37	---	16.10	---
	1174.43	---	16.10	---
	1178.00	1178.3	16.13	---
Si III (1) w,l	1206.51	1206.7	0.00	1.68
Si III (50) w,p	1212.01	1212.3	19.02	---
Si III (74) w,p	1212.25	1212.3	32.11	---
Si III (63) w,p	1280.35	1280.1	20.55	---
Si III	1294.54	1294.2	6.55	---
(4) w,p	1296.73	1296.0	6.54	---
	1298.89	---	6.55	1.80
	1298.96	---	6.58	
	1301.15	1300.8	6.55	0.40
	1303.32	---	6.58	0.50
Si III (10) w,p	1212.59	1312.0	10.28	---
Si IV	1045.50	1045.6	27.06	---
(21) w,p	1047.27	1048.2	27.08	---
Si IV (K) w,p	1051.60	1051.1	---	---
Si IV (11) m	1066.63	1066.4	19.88	---
Si IV	1122.49	1122.5	8.84	1.8
(3) m	1128.32	1127.9	8.90	0.2
	1128.34		8.90	1.0
Si IV	1210.65	---	24.05	---
(16) w,p	1211.76	1212.2	24.05	---
Si IV	1280.34	1280.2	---	---
(K) w,p	1291.97	1292.3	---	---
P III	998.00	998.7	0.00	---
(2) v,p	1003.59	1003.6	0.07	---
P III	1049.82		9.29	---
(K) w,l	1050.52	1051.0	9.29	---
	1050.82		9.29	---
P IV (1) w,l	950.67	951.1	0.00	2.75
P IV	1025.58	---	8.41	---
(2) w,p	1028.13	---	8.38	---
	1030.54	1030.3	8.47	---
	1033.14	---	8.41	---
	1035.54	---	8.47	---
P IV	1086.94	1086.3	23.47	---
(K) v,p	1088.61	1089.0	23.47	---
	1091.44	1091.0	23.47	---
P IV (K)	1118.59	1118.9	13.04	---
P IV (K) v,p	1161.78	1161.6	29.00	---
P IV (K) v,p	1197.82	1197.5	31.92	---
P IV	1203.41	1203.0	31.82	---
(K) v,p	1204.30	1204.9	31.81	---
	1206.51	1206.7	31.80	---
P IV (K) v,l	1264.48	1264.6	29.00	---
P V	997.64	997.3	25.31	---
(K) v,p	1000.36	1000.6	25.31	---
P V	1117.99	---	0.00	1.27
(H) m	1128.01	1127.9	0.00	0.63
S II	1250.50	1250.8	0.00	0.45
(1) i,v,p	1253.79	1254.2	0.00	0.89
	1259.53	1259.8	0.00	1.34
S III	1012.49	1012.5	0.00	0.30
(2) w,l	1015.51	1014.5	0.04	0.52
	1015.76		0.04	0.38
	1021.10	1121.3	0.10	0.38
	1021.32		0.10	1.12
S III (8) w,p	1077.84	1078.4	1.40	---
S III	1122.42	---	10.42	---
(K) v,p	1126.48	1126.7	10.41	---
	1126.85		10.42	---
S III	1155.34	1155.8	10.42	---
(K) v,p	1162.52	---	10.42	---
	1166.13	---	10.41	---
S III	1190.17	1189.7	0.00	0.42
(1) w,l	1194.02	1193.8	0.04	0.94
	1194.40		0.04	0.32
	1200.97		0.10	1.77
	1201.71	1200.2	0.10	0.32
	1202.10		0.10	0.021
S III	1328.12	1328.8	12.24	---
(K) v,p	1328.52		12.24	---
S IV	1062.67	1063.0	0.00	0.94
(1) w,l	1072.99	1073.0	0.12	0.19
	1073.52		0.12	1.69
S IV	1108.36	1108.0	15.31	---
(K) w,p	1110.90	1110.3	15.31	---
S IV (K) v,p	1138.23	1138.0	15.31	---
S IV	1286.06	1296.8	16.56	---
(K) v,p	1296.64	1296.0	16.64	---
S VI	933.38	928.8	0.00	0.5
(1) c		933.0		
	944.52	940.8	0.00	1.0
		945.2		
Cl III	1005.28	1005.0	0.00	0.56
(1) v,p	1008.78	1009.2	0.00	1.10
	1015.02	1014.5	0.00	1.66
Cl IV	973.21	---	0.00	0.55
(H) w,l	977.56	977.0	0.06	1.24
	977.90		0.06	0.42
	984.95	---	0.17	2.32
	985.75	---	0.17	0.44
Ar IV	1187.80	1187.8	4.32	---
(K) v,p	1190.35	1190.9	4.32	---
	1197.84	1197.5	4.32	---
Fe II (18) i,w,p	1096.89	1096.3	0.00	---
Fe II	1142.33	1142.2	0.00	---
(10) i,v,p	1143.24	---	0.00	---
	1144.95	1144.8	0.00	---
Fe III	1122.53	1122.5	0.00	4.50
(1) w,l	1124.88	1124.8	0.05	2.32
	1126.72	---	0.09	0.88
	1128.02	1127.9	0.05	1.17
	1128.72	---	0.09	1.46
	1129.19	---	0.12	1.12
	1130.40	---	0.13	0.50
	1131.19	1131.6	0.12	0.38
	1131.91		0.09	0.17
Fe IV	1254.80	---	20.86	---
(K) w,p	1257.29	---	20.89	---
	1258.68	---	20.89	---
	1259.54	1259.8	20.93	---
	1261.72	---	21.00	---
	1263.47	---	20.93	---
	1265.28	---	21.09	---
	1268.40	1268.3	21.00	---
	1271.08	1271.6	21.21	---
	1273.49	1273.0	21.09	---
	1280.43	---	21.21	---

* The eye estimated strength of the feature is strong, s; moderate, m; weak, w; or very weak, v.
/ The suggested identification is likely, l; or possible, p.
≠ The feature appears as a P Cygni type profile, c; or is probably interstellar in origin, i.

1970ApJ...160..595S

to the compilations of Moore (1950, 1965), a K refers to the emission line tables of Kelly (n.d., 1968), an H indicates that the paper of Hickok and Morton (1968) was used, P refers to an article of Palenius (1967), and HA refers to the work of Hallin (1966). Laboratory-measured wavelengths of the identified transitions and the observed wavelengths of the corresponding spectral features are listed in columns (2) and (3), respectively, and the excitation potentials in column (4). For those transitions exhibiting P Cygni–type profiles, column (3) lists the wavelength at the center of the absorption component followed by the wavelength corresponding to the blue emission edge. Listed in column (5) are *gf*-values taken from Varsovsky (1961), Allen (1963), Wiese, Smith, and Glennon (1966), and Garstang and Shamey (1967). No blends have been indicated simply because most lines are observed to be blends of two or more plausible transitions, and in those cases where only one transition correlates with an observed feature it is likely that other as-yet-unrecognized transitions do as well.

IV. DISCUSSION

The following paragraphs contain remarks on the lines of the various ions identified in the recorded spectra.

a) H I

Most of the absorption in the Lyman lines must be due to interstellar hydrogen. All the Lyman lines through Lθ except Lα and Lδ are masked by much stronger lines in the spectrum.

b) He II

The transition at 949.3 Å may contribute to the feature near 949.9 Å. All other transitions throughout the measured spectrum are masked to some extent by stronger absorption and emission features. No emission in He II can be identified.

c) C I, C II, C III, C IV

Of the six resonance lines in C I listed in Table 2 for which some evidence is found, the identification of only two at 1277.2 and 1280.2 Å can be considered probable.

There is mediocre evidence for two resonance lines in C II at 1036.3 and 1334.5 Å which are presumably interstellar in origin. The well-observed C III (1175.7 Å) line is seen as a P Cygni profile with weak emission, and modified by the unshifted absorption line. The same kind of profile might be expected at 977.0 Å, where a resonant transition in C III exists. Evidence for an unshifted absorption line at this wavelength is good, but the expected P Cygni profile will be masked by other absorption lines and bands. The unshifted, subordinate lines of C III at 1175.7, 1247.4, and 1296.3 Å originate in the stellar atmosphere, and in the case of the 1175 .7Å line the optical depth at this wavelength in the circumstellar envelope is not sufficiently large to prevent seeing to the "surface" of the star.

There is weak evidence for C IV near 1108.0 Å. Weak lines near 1169.0 and 1198.6 Å might be expected; however, in both cases strong absorption from C III (1168.8 Å) and N I (1199.9 Å) predominate in the respective wavelength regions. The lines of C IV at 948.1 and 948.2 Å are also not observed. The highest excitation observed in any of the carbon ions is 39.5 eV in C IV.

d) N I, N II, N III, N IV, N V

Preliminary calculations show that the N I lines at 1134.6 and 1199.9 Å must be telluric as well as interstellar in origin.

The absorption feature at 1084.3 Å is probably due to the combined effect of N II (1084.0 Å), a resonance transition, and He II (1085.0 Å). It is improbable that N II is abundant in the stellar atmosphere, and, since the ionization potential of N I is 14.5 eV, it is also improbable that N II will occur in the H I regions of interstellar space. Thus, almost all of the N II producing the feature at 1084.3 Å must be located in the H II region surrounding ζ Pup.

The N III doublet at 991.0 Å originates in the ground-state configuration, and exhibits a P Cygni profile with the emission and absorption features probably influenced by telluric N_2 and Cl III absorption, respectively. The weak unshifted absorption features identified in Table 1 with subordinate lines in this ion must arise within the stellar atmosphere.

There is considerable evidence in the spectrum for the existence of subordinate lines of N IV, and these are listed in Table 1. Such lines at 1168.6, 1169.1, and 1169.5 Å for which poor evidence exists are masked by shifted C III (1175.7 Å) absorption at 1168.8 Å. The transition at 955.3 Å exhibits a relatively weak P Cygni profile. The lower level is at 16.1 eV, and may decay radiatively to the ground state ($2p\ ^1P^o \rightarrow 2s^2\ ^1S$) with $gf =$ 0.64. The most likely way that the $^1P^o$ level may be populated is by ordinary thermal processes. This implies that the radiation field cannot be significantly diluted, and that the excited N IV ions must therefore be close to the "surface" of the star. Morton (1969) has also reached this conclusion. A multiplet of N IV at 923.2 Å is mainly responsible for terminating the observed spectrum near 921 Å; it should also exhibit a P Cygni profile. The range in observed excitation of atmospheric N IV is large, extending from 23.3 to 61.7 eV.

Perhaps the strongest feature of the recorded spectrum is the circumstellar P Cygni–type profile of N V (1238.8, 1242.8 Å). On the other hand, the evidence for the subordinate lines of N V at 1049.6 and 1048.2 Å is weak but, if accepted, indicates the highest observed state of excitation, namely, 76.3 eV.

e) O III, O IV, O VI

Evidence for only four subordinate lines of O III as listed in Table 2 has been found, the maximum observed excitation in this ion being 26.1 eV.

The O IV lines at 1338.6, 1343.0, and 1343.5 Å are strong and show a displacement to shorter wavelengths; apparently there is a small redshifted emission feature associated with the 1343.0–1343.5 Å transition. As in the case of the N IV (955.3 Å) P Cygni profile, this transition originates in an excited level of 22.3 eV which can decay radiatively to the ground state ($2p^2\ ^2P \rightarrow 2p\ ^2P^o$) with $gf = 2.28$. If the population of the 22.3-eV level is by thermal processes, then the excited O IV ions must be close to the "surface" of the star.

The P Cygni–type profile near 1030 Å associated with the resonance lines of 1031.9 and 1037.6 Å in O VI is nearly as strong as the P Cygni profile associated with the 1238.8 and 1242.8 Å lines in N V. The profile is modified by absorption of interstellar C II at 1036.3 Å, and possibly by a P IV line at 1031 Å. If the influence of the latter is small, it is likely that the absorption components of the doublet are partially resolved, and the profile may prove useful for an estimate of mass loss.

f) Si II, Si III, Si IV

Lines in Si II at 1260.4 and 1304.4 Å are definitely observed, and are likely to be interstellar in origin. Their profiles, however, are modified by line absorption at nearby wavelengths, and estimates of the interstellar abundance of Si II are unreliable. Other resonance lines in this ion appear at 1190.4 and 1193.3 Å, but their identification is uncertain.

The resonant Si III line at 1206.5 Å appears as a weak but definite absorption line in these data, but cannot plausibly be associated with a shortward-shifted feature at 1200 Å as suggested by Morton, Jenkins, and Brooks (1969). The latter feature certainly exists, but can be attributed exclusively to the combined effect of interstellar and telluric absorption in N I and absorption in three lines near 1201 Å originating in the ground-state configuration of S III. The plentiful, weak subordinate lines in Si III are listed in Table 2, and exhibit a range in excitation extending from 6.5 to 32.1 eV.

Relatively strong subordinate lines in Si IV are found in one multiplet at 1128.3 and 1122.5 Å, and in another at 1066.6 Å. The four other tentatively identified multiplets of this ion contain weak lines with excitation extending to 27.1 eV. No resonance lines of Si IV are found in the recorded wavelength region.

g) P III, P IV, P V

There is some evidence for ground-state transitions in P III at 998.0 and 1003.6 Å; however, the doublet in this ion at 1334.8–1344.9 Å is probably masked by the effects of interstellar C II and circumstellar O IV absorption. There is only one other tentatively identified multiplet of P III near 1051 Å, the excitation being 9.3 eV.

The resonance line in P IV at 950.7 Å very likely contributes to the feature at 949.9 Å together with transitions in H I (Lδ) and He II (949.3 Å). The P IV lines at 1030.5 and 1035.5 Å may contribute to the features near these wavelengths, but it is thought that these features are predominately due to shortward-shifted O VI absorption at 1037.6 Å and interstellar absorption in C II at 1036.3 Å, respectively. The remaining weak lines in P IV indicate a maximum observed excitation of 31.9 eV.

Resonance transitions in P V have reliably been identified at 1118.0 and 1128.0 Å, and subordinate lines indicating 25.3 eV of excitation in P V have tentatively been identified at 997.6 and 1000.4 Å.

h) S II, S III, S IV, S VI

There is weak evidence for interstellar S II where resonance transitions occur near 1255 Å.

Good evidence exists for the presence of the resonance transitions in S III near 1020 and 1200 Å. Generally, mediocre evidence for subordinate lines in S III exists which indicates a maximum observed excitation of 12.2 eV.

Ground-state transitions in S IV at 1063 and 1074 Å are clearly seen, but appear to be considerably weaker than the corresponding lines in the model spectrum. The discrepancy most likely illustrates the difficulty in determining the proper damping constants to use in model calculations. Subordinate lines in S IV reveal a maximum observed excitation of 16.6 eV. The strongest features due to sulfur, however, arise in the circumstellar envelope, and are the P Cygni–type profiles associated with the transitions in S VI at 933.4 and 944.5 Å.

i) Cl III, Cl IV

The resonance lines in Cl III near 1010 Å are weak if indeed detectable. Three lines at 985.8, 985.0, and 973.2 Å in Cl IV which should be observable are likely to be masked by the N III (989.8, 991.6 Å) P Cygni profile and a strong telluric N_2 (972.1 Å) band. It is also likely that the shape of the spectrum near 977.0 Å where ground-state transitions in Cl IV (977.6, 977.9 Å) may produce some observable effect is determined chiefly by the strong resonance transition in C III at 977.03 Å.

j) Ar IV

Mediocre evidence for transitions in Ar IV ions with an excitation of 4.3 eV is noted near 1187.8, 1190.4, and 1197.8 Å.

k) Fe II, Fe III, Fe IV

The only plausible evidence for Fe II, presumably of interstellar origin, is near 1142 Å and possibly 1096 Å. Other possible resonance lines either do not correspond to features in the spectrum or correspond to features primarily due to other ions.

There is good evidence in the spectrum for transitions from the ground-state configuration in Fe III at 1124.9 Å. The *gf*-value of the resonance transition at 1122.5 Å is about twice that for the 1124.9 Å transition; consequently, the resonance transition probably contributes to the moderate absorption feature at 1122.5 Å.

A multiplet of Fe IV near 1270 Å is the only apparent evidence for this ion throughout the observed spectral range which includes no resonance lines. The excitation of the ion for the observed multiplet is close to 21 eV.

Some features which are likely to be caused by some absorption agent but for which none at all could be found are listed in Table 3. Notable are two weak emissionlike features at 1226.5 and 1094.2 Å which seem to have some correlation with similar features on the short exposure. If these are not spurious effects, no plausible explanations can be made at the present time.

TABLE 3

UNIDENTIFIED LINES IN THE ULTRAVIOLET SPECTRUM OF ζ PUPPIS

λ (Å) Measured	λ (Å) Measured	λ (Å) Measured	λ (Å) Measured
1357.7 m*	1306.5 w	1221.5 v	1091.0 v
1352.8 w	1266.0 w	1104.7 v	1080.0 v
1350.0 w	1257.7 w	1102.6 v	1075.7 v
1346.1 w	1226.5 e	~1100† v	1017.7‡ v
1320.8 w	~1225 v	1094.7 v	1000.6 v
1311.7 w	1222.9 v	1094.2 e	

* The strength of the feature is moderate, m; weak, w; very weak, v; the feature appears in emission, e.

† The feature is a blend of weak lines.

‡ This line may be due to H_2O.

TABLE 4

CHARACTERISTIC RADIAL VELOCITIES OF IONS IN THE CIRCUMSTELLAR ENVELOPE OF ζ PUPPIS

Ion	C III	N III	N IV	N V	O IV	O VI	S VI
Laboratory wavelength (Å)....	1175.7	989.8 991.5 991.6	955.3	1238.8 1242.8	1338.6 1343.0 1343.5	1031.9 1037.6	933.4 944.5
Central velocity (km sec^{-1})....	1760 (1860)	1820	530 (780)	1670 (1550)	150	1830	1380
Extrapolated maximum velocity (km sec^{-1})................	3200	3300	1500	3300	1300	3500	2500

Summarized in Table 4 are the data concerning the P Cygni–type profiles measured in the present experiment.

For the purposes of this table only the velocities derived from the profile corresponding to the 933.4 Å transition in S VI are listed. The emission associated with this transition would cause an underestimation of the mean radial velocity of S VI ions as determined from the shortward-shifted 944.5 Å absorption line. The contributions of the Cl IV (985 Å) line to the N III (991 Å) profile and a P IV multiplet near 1031 Å to the O VI (1032, 1038 Å) profile have been assumed negligible. The extrapolated maximum velocities are of course quite uncertain.

Morton, Jenkins, and Brooks have determined radial velocities for three of the ions contained in Table 4; their results appear in parentheses and indicate substantial agreement with the present results. In the case of N IV it is noteworthy that these authors observed a transition at 1719 Å which originates at the same excited level ($2p\ ^1P^o$, 16.13 eV) as does the 955 Å transition reported here.

For the purpose of calculating the columnar density of atomic hydrogen the calibration curve of Figure 1 was used to obtain the relative flux distribution in the wavelength interval between 1194 and 1236 Å. The results are given by the solid line in Figure 4. Other sources of line absorption including the shifted absorption component of the circumstellar N V (1239, 1243 Å) doublet have been identified) in the figure, and quite obviously pose a difficult problem in the determination of that part of the profile due

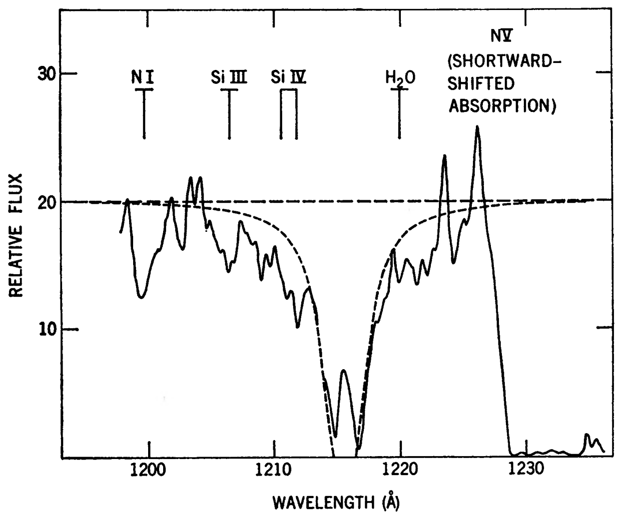

FIG. 4.—Lα line in the spectrum of ζ Pup. *Abscissa*, wavelength; *ordinate*, relative flux values. *Solid line*, measured relative flux distribution; *dashed contour*, a computed profile fitted to the observations in the core of the line. *Dashed horizontal line*, assumed position of the continuum.

exclusively to Lα absorption. In order to make this distinction the shape of the interstellar line was assumed to be of the form

$$I(\lambda)/I_0 = \exp\,[-CH(a, u)]\,, \qquad (1)$$

where I_0 is the flux in the stellar continuum, $H(a, u)$ is the Harris function, and C is defined by the relation

$$Nl = \frac{C}{\pi}\frac{mc}{e^2}\frac{\Delta\nu_0}{f}\,. \qquad (2)$$

Here, N is the mean number density of hydrogen atoms and l is the interstellar distance through atomic hydrogen. The other symbols in equations (1) and (2) have their usual meanings (Aller 1963). In the case of the heavily saturated Lα line the observed profile is determined essentially by radiation damping, the Doppler width $\Delta\lambda_0$ being very small, i.e., about 0.05 Å for a temperature of 10000° K. Thus, the exponent in equation (1) reduces to $(-)Ca/\pi u^2$, which is independent of temperature. On the assumption of a value for I_0, profiles for various values of C were computed, and the best value of C was selected on the basis of the best fit between the computed and measured profiles in the core of the Lα line. The dashed lines in Figure 4 illustrate the procedure showing both the assumed continuum and the best-fit computed profile. It was hoped that in this way the effects of line absorption in the vicinity of the interstellar Lα line could be significantly reduced.

Application of equation (2) gives the final result of $N = (7.6 \pm 2.5) \times 10^{19}$ cm^{-2}, the quoted error being due exclusively to the estimated uncertainty in establishing the continuum level. If the value for l of 390 pc suggested by Morton, Jenkins, and Brooks is adopted, N becomes (0.064 ± 0.021) cm^{-3}. The equivalent width is of interest when a comparison with other results is to be made. It can be easily deduced from the value of Nl, and is 6.4 Å.

V. SUMMARY AND CONCLUSIONS

Evidence for all the lines used in the Hickok and Morton model has been found except for those masked either by N_2 absorption bands or by strong P Cygni–type profiles. Some observed lines, however, appear to be considerably weaker than the corresponding model lines—the S IV doublet near 1070 Å is an example—and this circumstance most likely reflects an uncertainty in the damping constants to be used in the model calculations. All of these lines originate at ground or low-lying levels. Most of the identified features, however, correspond to subordinate lines which exhibit a wide range in both ionization and excitation. As an example, Table 2 shows that lines of N III (980 Å), N IV (1079 Å), and N V (1048, 1050 Å) originate at levels of 12.5, 53.0, and 76.3 eV, respectively. Further, it may be stated qualitatively that line blanketing from the weak lines in the observed spectral region is sufficient to affect the energy distribution in the spectrum. This is particularly noticeable in the wavelength intervals extending from 998 to 1015 Å and from 1190 to 1210 Å.

These results are in essential agreement with spectral observations carried out in the visible on stars of similar type. For example, N V has been identified in the spectrum of HD 190429 (O5f) by Swings and Struve (1940), again in the same star by Oke (1954), and in 9 Sge (O7) by Underhill (1958). In addition, Miss Underhill has tentatively identified the presence of O VI in 9 Sge. Both of these stars exhibit lines of N III and N IV, and in 9 Sge O III and O IV are definitely present while O V is probably present. Likewise, the range of excitation in the atmospheres of these stars is similar to that revealed in the ultraviolet spectrum of ζ Pup. Thus, the observed excitation of the N V ions in the atmosphere of HD 190429 extends from 56.3 to 59.0 eV, and the excitation of the O VI ions tentatively identified in 9 Sge is over 100 eV.

The similarity between the ultraviolet and visible observations may be carried further by noting that the excitation of N IV and Si IV ions revealed by the many ultraviolet lines is close to or equal to the excitation revealed in these ions by visible spectra. For example, the ultraviolet Si IV lines in the ζ Pup spectrum at 1211 and 1212 Å originate in the same lower level as the visible lines in the spectrum of 9 Sge (O7) at 4089 and 4116 Å; the excitation is 24.0 eV. Swings and Struve observed these last two lines as P Cygni–type profiles in HD 190429 (O5). Similarly, the N IV lines of ζ Pup at 1133 and 1136 Å originate in the same level as the visible lines at 3479–3985 Å in the spectra of both 9 Sge and HD 190429; the excitation in this case is 46.6 eV. If we neglect the possibility of a time variation in spectral characteristics and avoid wavelengths where strong absorption occurs, we can plausibly conclude that in both the ultraviolet (921–1360 Å) and the visible we see to atmospheric levels with physical parameters sufficiently similar to produce identical ions. The geometrical extent of the atmosphere over which the appropriate physical parameters exist is probably large; nevertheless, these results are consistent with the fact that the principal source of continuous opacity in the early O stars is free-electron scattering and thus varies only slowly with wavelength.

No evidence has been found for narrow unshifted emission lines similar to those of He II (4686 Å), N III (4634, 4642 Å), and C III (5696 Å) characteristic of Of stars in this or any other ultraviolet spectrum of ζ Pup. A probable explanation is that no selective-excitation processes, such as the familiar fluorescence mechanisms which require large fluxes of He II and H I Lα quanta, are operating at wavelengths less than 1965 Å. As one might expect, however, it is very difficult to establish a suitable continuum flux level, and consequently it is impossible to detect weak emission in the present data with reasonable certainty.

It was pointed out in § IV that the P Cygni profiles produced in N IV ions near 955 Å and in O IV ions near 1340 Å very likely arise close to the stellar atmosphere where dilution effects are still weak. The mean radial velocities of these ions are relatively small, 530 and 150 km sec^{-1}, respectively. On the other hand, the lower level of the transition associated with the P Cygni profile in C III near 1176 Å is metastable. It can be populated only under conditions where the radiation field is dilute, that is, when the C III ions are at distances on the order of several stellar radii from the center of the star. In distinction with the excited N IV and O IV ions, the C III ions possess a relatively large mean radial velocity of 1760 km sec^{-1}. It may also be noted that from any plausible atmospheric temperatures and pressures there should be no appreciable atmospheric abundances of N V or O VI, and yet the data indicate a large abundance of these ions in the circumstellar envelope. It is reasonable to assume that N V and O VI with mean radial velocities close to 1800 km sec^{-1} occur with maximum probability well beyond the unaccelerated atmosphere where suitable conditions exist, that is, high electron temperatures and low electron densities when compared with photospheric values. These data are usually interpreted as evidence for a positive velocity gradient in the detectable part of the circumstellar envelope.

Table 4 shows that not only do ground-state ions observed in the circumstellar envelope possess escape velocities, but their mean radial velocities (with the exception of S VI) are comparable; the average is 1770 km sec^{-1}. Ions of C III in the metastable state at 6.5 eV have a mean radial velocity of 1760 km sec^{-1}, nearly identical with the average of the ground-state ions. In addition to the values quoted in Table 4, Morton, Jenkins, and Brooks have measured mean radial velocities of 1840 and 1810 km sec^{-1} for the ions of C IV and Si IV, respectively. Their average mean radial velocity for ground-state ions is 1730 km sec^{-1}. The similarity of these results, including both the ground-state ions of C IV, N III, N V, O VI, and Si IV and the excited C III ions, is noteworthy, particularly when it is realized that the density distribution with distance from the star of each ion can well account for the velocity differences between ions. It should also be noted that the difficulty in establishing the position of the minimum residual intensity in the shifted absorption feature will produce at best an uncertainty in the corresponding velocity estimate of ± 100 km sec^{-1}. For the highly saturated lines this uncertainty is larger. The deficit in the mean radial velocity of S VI ions when compared with the average value is 390 km sec^{-1}. It may be due to the influence of some unrecognized source of absorption or emission near the S VI (933, 945 Å) lines, the density distribution of these ions in the circumstellar envelope, or a combination of both effects. The deficit, however, may occur for some entirely different reason, and this uncertainty reflects a rather unsatisfactory understanding of the circumstellar envelope. In spite of the anomalous characteristic of the S VI lines, the data suggest that the excaping ions are at least loosely bounded together in a circumstellar plasma with essentially no difference in the average acceleration of the various individual particles.

It is probable that the degree of ionization increases with increasing distance from the stellar surface but the lower levels of ionization as evidenced by the strong N III P Cygni profile at 991 Å are not completely depleted. The C III (977 Å) transition should also be seen as a P Cygni profile since the ionization potentials of N III and C III are about the same, that is, 47.2 and 47.7 eV, respectively. The data are indeed consistent with this prediction, but are as noted in § III confused by the presence of a telluric N_2 absorption band. On the other hand, the Si III (1207 Å) resonance line is not seen in the present observation as a P Cygni profile. The ionization potential for this ion is 33.3 eV, and on the basis of these facts one would not expect to find S III (ionization potential 34.9 eV) ions in the interstellar envelope, but would find O III (ionization potential 54.7 eV) ions there. It is reasonable to expect that N IV exists in the ground state at roughly the same distances and velocities as N III and N V. We do not detect it because the resonance transitions lie at wavelengths less than 912 Å which are hidden from view by interstellar atomic hydrogen. For the same reason the ions of C V, O III, O IV, and O V, which can be expected in the circumstellar envelope, cannot be observed.

Again, the visual data and the ultraviolet data can be considered self-consistent with respect to emission lines and P Cygni profiles. The visible emission lines characteristic of Of stars very likely originate high in a hot rarefied atmosphere (Oke 1954), yet with a geometrical dilution factor still close to unity. These same lines may possess a broad, weak emission component with a maximum extent corresponding to radial-velocity values in excess of 1000 km sec^{-1} in λ Cep (O6f) (Wilson 1958), and from 500 to 1000 km sec^{-1} in 9 Sge (O7) (Underhill 1958). In the latter case the N III (4634–4640 Å) line seems to appear as a P Cygni–type profile, and in the case of HD 190429 (O5f) Swings and Struve have noted P Cygni–type profiles of high-excitation lines in N IV (4057 Å), N V (4603, 4619 Å), and Si IV (4098, 4116 Å) with radial-velocity values of 182, 169, and 161 km sec^{-1}, respectively. These features arise presumably beyond the levels wherein the sharp characteristic lines are formed in a region where radial acceleration of the atmosphere has already begun. Here the N IV lines at 955 and 1719 Å and the O IV lines at 1339 and 1344 Å are also formed. Further out where the dilution factor has decreased significantly, population of the ionic ground states is preferred. However, even at these distances, perhaps 2 and 3 stellar radii from the center of the star, there is some excitation as evidenced by the spectrum of λ Cep.

The mean density of hydrogen atoms in the H I region between the Sun and ζ Pup was determined to be (0.064 ± 0.021) cm^{-3}, which is a factor of 3.1 smaller than the value of 0.2 cm^{-3} proposed by Field, Goldsmith, and Habing (1969) for the density of intercloud nuclei. The observed value might reasonably be raised to 0.106 cm^{-3} by taking into account both the uncertainty in locating the continuum and the uncertainty in the contour-fitting method described in § IV. On the other hand, the interstellar distance through atomic hydrogen (390 pc) may be too large. In view of these uncertainties it is concluded that the observed and model densities are at least consistent with each other, neither being implausible.

I wish to thank Messrs. A. K. Stober, J. L. Shannon, and R. Scolnik for their great assistance both in preparing the instrument and in the launch and recovery operations. The success of the experiment was also due in part to the efforts of the personnel in the Sounding Rocket Branch of the Goddard Space Flight Center, and particularly to Mr. T. Collinson who was primarily responsible for the proper functioning of the attitude control system.

REFERENCES

Allen, C. W. 1963, *Astrophysical Quantities* (2d ed.; London: Athlone Press).
Aller, L. H. 1963, *The Atmospheres of the Sun and Stars* (2d ed.; New York: Ronald Press), p. 323.
Field, G. B., Goldsmith, D. W., and Habing, H. J. 1969, *Ap. J.* (*Letters*), **155**, L149.
Fowler, W. K., Rense, W. A., and Simmons, W. R. 1965, *Appl. Optics*, **4**, 1596.
Garstang, R. H., and Shamey, L. J. 1967, in the *Magnetic and Related Stars*, ed. R. C. Cameron (Baltimore: Mono Book Corp.).
Hallin, R. 1966, *Ark. f. Fys.*, **31**, 511.
Hickok, F. R., and Morton, D. C. 1968, *Ap. J.*, **152**, 203.
Kelly, R. L. n.d., *Table of Emission Lines in the Vacuum Ultraviolet for all Elements*, University of California Radiation Laboratory, publication 5612.
———. 1968, *Atomic Emission Lines Below 2000 Angstroms*, U.S. Naval Research Laboratory Report 6648.
Moore, C. E. 1950, *N.B.S. Circ.*, No. 488, § 1.
———. 1965, *N.S.R.D.S.-N.B.S.*, No. 3, § 1.
Morton, D. C. 1969, *Ap. and Space Sci.*, **3**, 117.
Morton, D. C., Jenkins, E. B., and Brooks, N. H. 1969, *Ap. J.*, **155**, 875.
Oke, J. B. 1954, *Ap. J.*, **120**, 22.
Palenius, H. P. 1967, *Ark. f. Fys.*, **34**, 571.
Smith, A. M. 1969, *Ap. J.*, **156**, 93.
Swings, P., and Struve, O. 1940, *Ap. J.*, **91**, 546.
Underhill, A. B. 1958, *Pub. Dom. Ap. Obs.*, **11**, 143.
Varsovsky, C. M. 1961, *Ap. J. Suppl.*, **6**, 75.
Wiese, W. L., Smith, M. W., and Glennon, B. M. 1966, *N.S.R.D.S.-N.B.S.*, No. 4.
Wilson, R. 1958, *Publ. Roy. Obs. Edinburgh*, Vol. **2**, No. 3.